Research Article

Igor V. Bodrenko*, Stefan Milenkovic, Matteo Ceccarelli

Diffusion of molecules through nanopores under confinement: Time-scale bridging and crowding effects via Markov state model

https://doi.org/10.1515/bmc-2022-0019
received January 31, 2022; accepted March 14, 2022

Abstract: Passive transport of molecules through nanopores is characterized by the interaction of molecules with pore internal walls and by a general crowding effect due to the constricted size of the nanopore itself, which limits the presence of molecules in its interior. The molecule–pore interaction is treated within the diffusion approximation by introducing the potential of mean force and the local diffusion coefficient for a correct statistical description. The crowding effect can be handled within the Markov state model approximation. By combining the two methods, one can deal with complex free energy surfaces taking into account crowding effects. We recapitulate the equations bridging the two models to calculate passive currents assuming a limited occupancy of the nanopore in a wide range of molecular concentrations. Several simple models are analyzed to clarify the consequences of the model. Eventually, a biologically relevant case of transport of an antibiotic molecule through a bacterial porin is used to draw conclusions (i) on the effects of crowding on transport of small molecules through biological channels, and (ii) to demonstrate its importance for modelling of cellular transport.

Keywords: nanopores, diffusive transport, molecular current, saturation, Markov state model

*** Corresponding author: Igor V. Bodrenko,** CNR/IOM, Section of Cagliari, c/o Department of Physics, S.P. Monserrato-Sestu km 0.700, 09042 Monserrato, Italy; Department of Life Sciences and Chemistry, Jacobs University Bremen, Campus Ring 1, 28759 Bremen, Germany, e-mail: igor.bodrenko@cnr.it
Stefan Milenkovic: CNR/IOM, Section of Cagliari, c/o Department of Physics, S.P. Monserrato-Sestu km 0.700, 09042 Monserrato, Italy
Matteo Ceccarelli: CNR/IOM, Section of Cagliari, c/o Department of Physics, S.P. Monserrato-Sestu km 0.700, 09042 Monserrato, Italy; Department of Physics, University of Cagliari, S.P. Monserrato-Sestu km 0.700, 09042 Monserrato, Italy

Introduction

Biological nanopores in eukaryotic and prokaryotic cells represent, for those molecules for which cell membranes are impermeable, the gate to diffuse in and out of and between internal organelles [1–3]. Specialized protein complexes provide the necessary modulation to the number of transported molecules (the flux/current) and their molecular characteristic (the selectivity). The main objective of a controlled and selective transport is to keep the integrity of the internal environment (membrane potential, concentrations of solutes, pH), key for a correct functioning of cells.

The main general and simple selection rule to achieve controlled transport is based on constriction of the pore size, where an entropic barrier prevents fast entry of molecules. The entropic barrier can be modulated independently by electrostatic and other specific chemical interactions. In biology, a typical example is provided by porins, beta-barrel proteins with an internal water-filled pore. In porins, the diffusive transport of molecules/ions/water is modulated by a constricted shape created by one or more loops folded internally and with different degrees of flexibility [4–7]. Investigating the transport of particles under confinement is thus of primary importance to unveil and rationalize the mechanism of biological nanopores functioning [8,9]. At the same time, such biological complexes are a source of inspiration for the development of artificial pores with potential technological applications, such as in molecular sensing [10–13].

Recently, the necessity to rationalize and predict the accumulation of molecules in Gram-negative bacteria has emerged as prerequisite to the development of new effective drugs [14,15]. For many small and polar molecules, their accumulation is obtained via a subtle balance between passive diffusion through porins (in and out) and active efflux (out) [16]. Experimentally the accumulation seems not to follow neither simple Fick's law kinetics for entry nor the Michaelis–Menten kinetics for extrusion [17,18], showing a nonlinear behavior. The Fick's law was first introduced to describe the free diffusion of noninteracting

Open Access. © 2022 Igor V. Bodrenko *et al.*, published by De Gruyter. This work is licensed under the Creative Commons Attribution 4.0 International License.

solute molecules in solvent and then generalized, by introducing the potential of mean force, to the case of membranes with pores, assuming linear concentration dependence. Thus, a proper treatment of saturation due to the interaction of the solute molecules is necessary for the correct use of Fick's law in a more general and complex model to understand and predict accumulation in finite volumes [15].

The passive transport of molecules through membrane pores is driven by the gradient of the chemical potential and can often be described within the diffusion approximation by using the over-damped Brownian dynamics or the Smoluchowski equation [19]. This model has been widely used for over a century in the form of Nernst–Plank equation for electrodiffusion. It is also behind important classical concepts of membrane physiology such as the membrane potential and current (Goldman–Hodgkin–Katz equation). This is a linear theory that assumes the linear dependence of the molecular flux through the pore on the concentration of the molecules and explains the generalized Fick's law of the permeability through membranes. The diffusion model also assumes that molecules do not interact with each other inside pores. In other words, it is valid at low concentrations when the probability to have two or more molecules in the pore at the same time is negligible. At high substrate concentrations, especially in the case of favorable pore–substrate interactions, the probability to have two substrate molecules trying to occupy the pore at the same time is not negligible. That leads to the slower growth of the diffusion current vs the substrate concentration, and finally to the saturation, i.e., the independence of the passive current on the concentration.

The saturation can be observed in single-channel electrophysiology (SCE) [20], where the presence of a molecule in the pore is detected via the observations of the corresponding blockages of the ionic current through the pore [21] or via the analysis of the ion current fluctuations at various concentration gradient [20]. The SCE data have been analyzed in terms of the Markov state model, [22], which assumes one or more binding sites for the molecule in the pore and uses the master equations, a discrete Markov process (Markov chain) model, to trace the time course of the occupation probabilities of the binding sites. The simplest two-state Markov model assumes that, at the maximum, one particle at a time can occupy the channel (binding site). It can describe both the linearity with the concentration and the saturated behavior. The parameters of the Markov state model, the transition rates between the states, in principle, can be obtained from the experiment (e.g., electrophysiology). In many cases, it is impossible to calculate directly the transport of molecules through nanopores by using the all-atom molecular dynamics (MD) simulations as the characteristic times (more than milliseconds) are beyond the capabilities of modern high-performance computing (HPC) infrastructures

However, thanks to the use of sophisticated algorithms for accelerating sampling, it is feasible to obtain the free energy surface for the transport of a molecule through a nanopore as well as the diffusion coefficient by using MD simulations and 1–100 microseconds long trajectories [23]. This gives the necessary input data for the diffusion model. In the present work, we discuss in detail how to exploit the free energy surface and the diffusion coefficient of the 1D diffusion model to obtain the rate constants of the corresponding Markov state model. Only by combining the two models, one can obtain the passive current of molecules through pores as function of the gradient concentration (or gradient of chemical potential), which can be accessed experimentally, for example, by the reversal potential method [23], thus also helping the interpretation of experimental results.

The mathematical grounds and physical applications of the continuous and discrete Markov processes have been known for decades if not centuries. However, the applications to the passive transport of molecules through nanopores bridging the timescales from the diffusion (ps-ns) to the Markov state (us-ms) are relatively recent, see, e.g., [24,25], and are mainly focused on the theoretical development based on the mean first passage time (MFPT) concept and to the analysis of simplified analytic models. Here, we focus on passive transport through biological nanopores within the bridged multiscale approach – from all-atom MD simulation to the 1D diffusion and two state Markov model (MD-1DD-2MS).

This article is organized as follows. First, we recapitulate the necessary results of the 1D diffusion theory and of the Markov state models. Then, we derive the expression of the kinetic rate constants in terms of the free energy profile and the diffusion coefficient, in original way, without the use of the MFPT concept. We discuss the qualitative properties of the theory on simple analytic models of free energy barriers and binding site and then consider, as a more realistic application, the transport of biologically related molecules through bacterial porins.

Theory

Diffusion model

In many cases, the transport of molecules though nanopores can be adequately described within the diffusion

approximation by considering the molecules as overdamped Brownian particles [19,26,27], and assuming the adiabatic separation of the time scales, i.e., the fast degrees of freedom are in the thermodynamic equilibrium, while few slow ones are evolving quasi-stationary according to a stochastic Markov process. Often, it is sufficient to consider only one slow coordinate, e.g., the one characterizing the position of the molecule along the pore axis or the reaction path. The corresponding one-dimensional Fokker–Planck equation (FPE) for the probability density of molecule's coordinate, $\phi(x, t)$, is reduced to the Smoluchowski diffusion-drift equation,

$$\frac{\partial \phi(x,t)}{\partial t} = \frac{\partial}{\partial x} D(x) \left(\frac{\partial \phi(x,t)}{\partial x} + \frac{\phi(x,t)}{kT} \frac{\partial U(x)}{\partial x} \right), \quad (1)$$

where k stands for Boltzmann's constant, T is the temperature, and $D(x)$ is the position-dependent diffusion coefficient. $U(x)$ is called the potential of mean force (PMF) as it generates the mean drift force acting onto the Brownian particle, $f(x) = -\mathrm{d}U(x)/\mathrm{d}x$. The difference between the PMF values at two points, x and $x = 0$, equals the minimal thermodynamic (reversible) work required for moving the molecule from point $x = 0$ to x, $U(x) = \int_0^x f(x')\mathrm{d}x' = W_{\min}(x)$; here, we set $U(0) = 0$. According to the fundamental principles of thermodynamics [28], the minimal work required to change a parameter of a system while keeping it in the thermodynamic equilibrium, e.g., maintaining constant pressure, p, and temperature, T, is equal to the corresponding difference of the appropriate thermodynamic potential of the total system (particle plus medium), e.g., the Gibbs free energy $W_{\min}(x) = G(x, p, T) - G(x = 0, p, T) \equiv \Delta G(x)$; therefore, $U(x) = \Delta G(x)$. Equation (1) has a Boltzmann-type equilibrium (zero-flux) solution, determined by the PMF and independent on the diffusion coefficient,

$$\phi_{\mathrm{eq}}(x) = c_0 \exp(-U(x)/kT), \quad (2)$$

where c_0 is a constant dependent on the boundary conditions (the concentration of the molecules outside the pore).

As far as the PMF, $U(x)$, is used to characterize the distribution of the particles in the thermodynamic equilibrium, the timescales of the fluctuations of the variables are not important. The description is equivalent to the classical Gibbs distribution. When one uses the PMF, $U(x)$, in the diffusion-drift equation to treat the system out of the thermodynamic equilibrium, the adiabatic separation of x from all other degrees of freedom must be assumed, in general. Fortunately, this very strong condition may be softened and the validity of the Smoluchowski equation may be extended if one introduces an appropriate modified position-dependent diffusion coefficient, $D(x)$ [29–32]. Still, it is worth to remind that diffusion is a time-average concept with respect to the all-atom dynamics. It assumes Maxwell's distribution in the momentum space, so that the diffusion time scale is much larger than the corresponding momentum relaxation time of the particle, $t \gg \tau_p = DM/kT$, where D is the diffusion constant and M is the mass. For a typical biologically related small molecule ($M = 250$ Da, $D = 1\ \mathrm{nm}^2/\mathrm{ns}$), at room temperature, one obtains $\tau_p = 0.1$ ps.

In the practically important case of the steady-state, the particle distribution is time independent, $\phi(x, t) = \phi(x)$, but the diffusion current, I, is nonzero and depends on boundary conditions. In particular, if the molecular bulk concentration on one side of the pore (*cis* side, at $x = 0$) is c^{C} and on the other side of the pore (*trans* side, at $x = L$) is c^{T} and the diffusion current is determined by the Kramers-type formula [26]:

$$I_D = S \frac{c^{\mathrm{C}} \exp\left(\frac{U(0)}{kT}\right) - c^{\mathrm{T}} \exp\left(\frac{U(L)}{kT}\right)}{\int_0^L \exp\left(\frac{U(x)}{kT}\right) \frac{\mathrm{d}x}{D(x)}}, \quad (3)$$

where S is the cross section of the channel at the entrance of the pore (the active surface of the pore). The average number of (noninteracting) diffusing molecules in the pore reads:

$$N_c = \int_0^L \exp\left(-\frac{U(x) - U(0)}{kT}\right) \times \left(Sc^{\mathrm{C}} - I \int_0^x \frac{\exp\left(\frac{U(x') - U(0)}{kT}\right)}{D(x')} \mathrm{d}x', \right) \mathrm{d}x. \quad (4)$$

For small numbers, $N_c \ll 1$ (at low concentrations c^{C}), this quantity has the meaning of the probability to find a single molecule in the channel (channel occupancy), $q = N_c$.

For the specific cases, equation (3) has been known and practically used for many decades, e.g., the Fick's law for the diffusive current through membranes driven by the gradient of the concentration, the Goldman–Hodgkin–Katz equation for ionic current through membrane driven by the gradient of the electric potential and ion concentration difference, etc. The formula for the diffusion current is modified in the case when the radiation boundary conditions are more appropriate [33], or for a single particle in a periodic PMF driven by a constant force [19,34,35].

Equation (3) demonstrates that the PMF enters the current in the exponent, while the diffusion coefficient does only linearly: the dependence of the diffusion

current on the PMF is stronger. In many cases, the diffusion coefficient can be effectively taken as a constant, $D(x) \approx D^*$. If the PMF creates a large barrier in the constriction region, $U(x_c) \gg kT$, the integral in (3) may be restricted to a short interval, Δx, around the barrier position, and the diffusion current reads:

$$I = S(c^{\mathrm{C}} - c^{\mathrm{T}})D^* \exp(-U(x_c)/kT)/\Delta x. \tag{5}$$

This latter concept has been successfully applied recently to model the permeation of antibiotics through outer membrane channels of Gram-negative bacteria [7,36].

The central input quantities of the model, $U(x)$ and $D(x)$, may be determined microscopically by using individual trajectories from all-atom simulations including, e.g., the pore, the membrane, the solvent, and the molecules, see, e.g., [37–40]. For large molecules and strong interaction, the timescale for the particle to cross the pore increases and plain all-atom simulations may become unable to achieve statistically convergent results. Then, the enhanced sampling methods (e.g., the umbrella sampling [41] or the metadynamics [42,43]) may be utilized. But even when using the enhanced sampling, the all-atom approach is still often computationally demanding as multi-microseconds long trajectories may be required [23,44–46].

Markov state model

The Markov state kinetic model of the pore–molecule interaction, used, e.g., for the analysis of the channel gating in the electophysiology [47], starts with a set of states defined by different ionic conductance levels of the channel (the "bound states") due to the presence of substrate molecules. The transitions between these states are assumed to be much faster than the corresponding residence times. The ground state is the open-channel state (optionally, several) without any molecule inside. The transitions between the states are described as a discrete Markov process determined by the corresponding rate constants – the target parameters describing the pore–molecule interaction kinetics [22].

Here, we consider a one-binding-site (two-states) Markov model of the channel, the extension to the many-state model is straightforward.

$$\mathrm{C}(cis) \rightleftarrows [\,\text{binding site}\,] \rightleftarrows \mathrm{T}(trans). \tag{6}$$

Let p_o, p_b are the probabilities to have the open channel and a single molecule in the pore, correspondingly. In the Markov state model, one introduces the transition rates, λ_{ob}, λ_{bo}, between the two states of the pore occupation states, and the simultaneous rate equations:

$$\dot{p}_o = -\lambda_{ob} p_o + \lambda_{bo} p_b, \tag{7}$$

$$\dot{p}_b = -\lambda_{bo} p_b + \lambda_{ob} p_o. \tag{8}$$

Additional normalization condition, $p_o + p_b = 1$, reflects the physical assumption that only a single molecule a time can stay in the pore. Then, one introduces the kinetic rates, $k^{\mathrm{C}}_{\mathrm{off}}$, $k^{\mathrm{T}}_{\mathrm{off}}$, for the transition of the particle from the binding site to the "*cis*" and the "*trans*" sides of the channel, respectively, so that $\lambda_{bo} = k^{\mathrm{C}}_{\mathrm{off}} + k^{\mathrm{T}}_{\mathrm{off}}$. Also, one assumes that the "*cis*" and "*trans*" compartments are large reservoirs keeping the molar concentrations of the molecules at the sides of the channel invariant, respectively, c^{C} and c^{T}. Thus, one can write down, $c^{\mathrm{C}}k^{\mathrm{C}}_{\mathrm{on}}$ and $c^{\mathrm{T}}k^{\mathrm{T}}_{\mathrm{on}}$, for the transition of the particle from the "*cis*" side and from the "*trans*" side, respectively, onto the binding site in the channel, so that $\lambda_{ob} = c^{\mathrm{C}}k^{\mathrm{C}}_{\mathrm{on}} + c^{\mathrm{T}}k^{\mathrm{T}}_{\mathrm{on}}$. Besides, we define the following quantities, which can be determined in the electophysiology:

$$k_{\mathrm{off}} = k^{\mathrm{C}}_{\mathrm{off}} + k^{\mathrm{T}}_{\mathrm{off}}; \quad K^{\mathrm{C}} = \frac{k^{\mathrm{C}}_{\mathrm{on}}}{k_{\mathrm{off}}}; \quad K^{\mathrm{T}} = \frac{k^{\mathrm{T}}_{\mathrm{on}}}{k_{\mathrm{off}}}. \tag{9}$$

Below, we summarize necessary results from the two-state Markov model in the steady-state [22,47,48]. If the particles are added on the both sides at the concentrations, respectively, c^{T} and c^{C}, the steady-state probability to find a molecule in the channel reads,

$$p_b = \frac{c^{\mathrm{T}}K^{\mathrm{T}} + c^{\mathrm{C}}K^{\mathrm{C}}}{c^{\mathrm{T}}K^{\mathrm{T}} + c^{\mathrm{C}}K^{\mathrm{C}} + 1}. \tag{10}$$

The net current of molecules through the pore reads,

$$\begin{aligned} I_{\mathrm{C}\to\mathrm{T}}(c^{\mathrm{C}}, c^{\mathrm{T}}) &= p_b k^{\mathrm{T}}_{\mathrm{off}} - (1 - p_b)c^{\mathrm{T}}k^{\mathrm{T}}_{\mathrm{on}} \\ &= \frac{c^{\mathrm{C}}k^{\mathrm{T}}_{\mathrm{off}}K^{\mathrm{C}} - c^{\mathrm{T}}k^{\mathrm{C}}_{\mathrm{off}}K^{\mathrm{T}}}{1 + c^{\mathrm{T}}K^{\mathrm{T}} + c^{\mathrm{C}}K^{\mathrm{C}}}. \end{aligned} \tag{11}$$

With the aforementioned definition, the current is positive for the net transport from *cis* to *trans*, and it is negative for the opposite direction.

From the aforementioned results, and from the general requirements of the zero net particle current, in the case of the symmetric bulk solution on the sides of the channel (equal concentrations, no electric field gradient, etc.), $I_{\mathrm{C}\to\mathrm{T}}(c, c) = 0$, one arrives at the detailed balance condition for the transition rates,

$$k^{\mathrm{C}}_{\mathrm{on}}k^{\mathrm{T}}_{\mathrm{off}} = k^{\mathrm{T}}_{\mathrm{on}}k^{\mathrm{C}}_{\mathrm{off}}. \tag{12}$$

Thus, one finally obtains,

$$\begin{aligned} I_{\mathrm{C}\to\mathrm{T}} &= \frac{K^{\mathrm{T}}K^{\mathrm{C}}}{K^{\mathrm{T}} + K^{\mathrm{C}}} \frac{(c^{\mathrm{C}} - c^{\mathrm{T}})k_{\mathrm{off}}}{1 + c^{\mathrm{T}}K^{\mathrm{T}} + c^{\mathrm{C}}K^{\mathrm{C}}} \\ &= \frac{K^{\mathrm{T}}K^{\mathrm{C}}}{K^{\mathrm{T}} + K^{\mathrm{C}}} k_{\mathrm{off}}(1 - p_b)(c^{\mathrm{C}} - c^{\mathrm{T}}). \end{aligned} \tag{13}$$

Equation (13) shows that the molecular pore-translocation current obeys Fick's law for small concentrations only, $c^{\mathrm{T}}K^{\mathrm{T}} + c^{\mathrm{C}}K^{\mathrm{C}} \ll 1$,

$$I_{\mathrm{C}\to\mathrm{T}}|_{c^{\mathrm{C}},c^{\mathrm{T}}\to 0} = \frac{K^{\mathrm{T}}K^{\mathrm{C}}}{K^{\mathrm{T}} + K^{\mathrm{C}}}k_{\mathrm{off}}(c^{\mathrm{C}} - c^{\mathrm{T}}), \tag{14}$$

$$p_b|_{c^{\mathrm{C}},c^{\mathrm{T}}\to 0} = c^{\mathrm{T}}K^{\mathrm{T}} + c^{\mathrm{C}}K^{\mathrm{C}}. \tag{15}$$

In the opposite case of large concentrations, in contrast with the diffusion approximation, the molecular current saturates and reaches its maximum, $I^{\max}$.

$$\begin{aligned} I^{\max}_{\mathrm{C}\to\mathrm{T}} &= \frac{K^{\mathrm{T}}}{K^{\mathrm{T}} + K^{\mathrm{C}}}k_{\mathrm{off}} = k^{\mathrm{T}}_{\mathrm{off}} \\ I^{\max}_{\mathrm{T}\to\mathrm{C}} &= \frac{K^{\mathrm{C}}}{K^{\mathrm{T}} + K^{\mathrm{C}}}k_{\mathrm{off}} = k^{\mathrm{C}}_{\mathrm{off}}. \end{aligned} \tag{16}$$

Another important difference between the Markov state model and the diffusion model is that the diffusion molecular current is always symmetric with respect to the side of application of the concentration gradient, while the Markov state translocation current is symmetric only at small concentrations. In general, the translocation current depends on the side of application of the concentration gradient,

$$I_{\mathrm{C}\to\mathrm{T}}(c^{\mathrm{C}}, c^{\mathrm{T}}) \neq I_{\mathrm{T}\to\mathrm{C}}(c^{\mathrm{T}}, c^{\mathrm{C}}). \tag{17}$$

In the case of asymmetric solvent on *cis* and *trans* sides, due, e.g., to the different solvent activity or an applied electric potential for charged molecules, the definition of the *in*-rates should be modified, $\lambda_{ob} = c^{\mathrm{C}}\exp\left(\frac{\psi^{\mathrm{C}}}{kT}\right)k^{\mathrm{C}}_{\mathrm{on}} + c^{\mathrm{T}}\exp\left(\frac{\psi^{\mathrm{T}}}{kT}\right)k^{\mathrm{T}}_{\mathrm{on}}$. The constant $\psi = \mu - kT\ln(x)$ is the difference between the chemical potential of the particle and the logarithm of its molar fraction; it contains both the activity and the applied electric potential. The detailed balance condition, (12), remains, but the net translocation current becomes ψ-dependent (compared with equation (3) for 1D diffusion),

$$\begin{aligned} &I_{\mathrm{C}\to\mathrm{T}}(c^{\mathrm{C}}, \psi^{\mathrm{C}};\, c^{\mathrm{T}}, \psi^{\mathrm{T}}) \\ &\quad= \frac{K^{\mathrm{T}}K^{\mathrm{C}}}{K^{\mathrm{T}} + K^{\mathrm{C}}}k_{\mathrm{off}} \\ &\qquad\times \frac{c^{\mathrm{C}}\exp\left(\frac{\psi^{\mathrm{C}}}{kT}\right) - c^{\mathrm{T}}\exp\left(\frac{\psi^{\mathrm{T}}}{kT}\right)}{1 + c^{\mathrm{C}}\exp\left(\frac{\psi^{\mathrm{C}}}{kT}\right)K^{\mathrm{C}} + c^{\mathrm{T}}\exp\left(\frac{\psi^{\mathrm{T}}}{kT}\right)K^{\mathrm{T}}}. \end{aligned} \tag{18}$$

Interestingly, the maximum current at high concentration is given by the same equations (16).

Bridging 1D diffusion and the Markov state models

To connect the kinetic rates of the Markov state model with the PMF and the diffusion coefficient, one can consider the low concentration limit, where the both models are linear with the concentration. Similar arguments have been used by other authors, see, e.g., [24,25]. We also assume that the solute at concentration c is added from one side only, and the PMF has same value at the ends, $U(0) = U(L) = 0$. The linear-regime probability to find a particle in the channel when added only from the *trans* and only from the *cis* side, respectively, can be defined as follows:

$$q^{\mathrm{T}}(c) = cK^{\mathrm{T}}; \quad q^{\mathrm{C}}(c) = cK^{\mathrm{C}}. \tag{19}$$

The linear-regime particle current through the channel when added to one side (the same for *trans* and *cis*) at concentration gradient c, reads,

$$I_D(c) = cK^{\mathrm{C}}k^{\mathrm{T}}_{\mathrm{off}} = cK^{\mathrm{T}}k^{\mathrm{C}}_{\mathrm{off}}. \tag{20}$$

Quantities $q^{\mathrm{T}}(c)$, $q^{\mathrm{C}}(c)$ and $I_D(c)$ can be calculated within the diffusion model by using equations (3) and (4). Thus, by defining the following quantities:

$$R = \int_0^L \exp\left(-\frac{U(x) - U(0)}{kT}\right)\mathrm{d}x, \tag{21}$$

$$Q = \int_0^L \frac{\exp\left(\frac{U(x) - U(0)}{kT}\right)}{D(x)}\mathrm{d}x, \tag{22}$$

$$T_0 = \int_0^L \frac{\exp\left(\frac{U(x)}{kT}\right)}{D(x)}\int_0^x \exp\left(-\frac{U(x')}{kT}\right)\mathrm{d}x'\mathrm{d}x, \tag{23}$$

$$T_1 = \int_0^L \exp\left(-\frac{U(x)}{kT}\right)\int_0^x \frac{\exp\left(\frac{U(x')}{kT}\right)}{D(x')}\mathrm{d}x'\mathrm{d}x, \tag{24}$$

satisfying $RQ = T_0 + T_1$, one finds,

$$K^{\mathrm{T}} = \frac{q^{\mathrm{T}}(c)}{c} = S\frac{T_1}{Q}; \quad K^{\mathrm{C}} = \frac{q^{\mathrm{C}}(c)}{c} = S\frac{T_0}{Q}, \tag{25}$$

$$k^{\mathrm{T}}_{\mathrm{off}} = \frac{I_D(c)}{q^{\mathrm{C}}(c)} = \frac{1}{T_0}; \quad k^{\mathrm{C}}_{\mathrm{off}} = \frac{I_D(c)}{q^{\mathrm{T}}(c)} = \frac{1}{T_1}, \tag{26}$$

$$k_{\mathrm{off}} = I_D(c)\frac{q^{\mathrm{T}}(c) + q^{\mathrm{C}}(c)}{q^{\mathrm{T}}(c)q^{\mathrm{C}}(c)} = \frac{T_0 + T_1}{T_0T_1} = \frac{RQ}{T_0T_1}, \tag{27}$$

$$k^{\mathrm{T}}_{\mathrm{on}} = I_D(c)\frac{q^{\mathrm{C}}(c) + q^{\mathrm{T}}(c)}{q^{\mathrm{C}}(c)} = S\frac{R}{T_0}, \tag{28}$$

$$k_{\text{on}}^{\text{C}} = I_D(c)\frac{q^{\text{C}}(c) + q^{\text{T}}(c)}{q^{\text{T}}(c)} = S\frac{R}{T_1}. \tag{29}$$

The aforementioned formulas connect the Markov state model with the diffusion approximation. T_0, T_1 quantities are equal to the mean first passage times defined in refs [24,25].

The translocation current and the channel occupancy at higher concentrations can be calculated by using Markov state model results, equations (10) and (13). In particular, if the molecules are added from one side only, one finds,

$$p_b^{\text{C}}(c) = \frac{q^{\text{C}}(c)}{q^{\text{C}}(c) + 1}; \quad p_b^{\text{C}}(c) = \frac{q^{\text{T}}(c)}{q^{\text{T}}(c) + 1}, \tag{30}$$

$$I_{\text{C}\to\text{T}}(c) = \frac{I_D(c)}{q^{\text{C}}(c) + 1}; \quad I_{\text{T}\to\text{C}}(c) = \frac{I_D(c)}{q^{\text{T}}(c) + 1}. \tag{31}$$

It is worth to note again that the two-state Markov state is a time average concept with respect to the continuous diffusion approximation. It assumes that the average time spent by the molecule in each of the states is much larger than the average diffusion time required to cross the barrier between the states. The latter can be estimated as $\tau_D = \Delta l^2/D$, where Δl is the characteristic width of the barrier. Therefore, the conditions of the applicability of the 1DD-2MS bridging discussed earlier read,

$$\tau_{\text{res}} = \frac{1}{k_{\text{off}}} \gg \frac{\Delta l^2}{D}, \tag{32}$$

$$\tau_{\text{in}}^{\text{cis}} = \frac{1}{ck_{\text{on}}^{\text{C}}} \gg \frac{\Delta l^2}{D}, \tag{33}$$

$$\tau_{\text{in}}^{\text{trans}} = \frac{1}{ck_{\text{on}}^{\text{T}}} \gg \frac{\Delta l^2}{D}. \tag{34}$$

Only if the aforementioned conditions are satisfied, one can use the obtained kinetic rates (k_{on}, k_{off}) to trace the nonequilibrium kinetics of the molecule–pore interaction, e.g., the opening and closing time series at it is observed by the electrophysiology.

However, equations (31) for the steady-state tanslocation current are also valid at much weaker conditions. It assumes two main approximations. First, the current, e.g., from *cis* to *trans*, is presentable in the form (compared with equation (20)),

$$I_{\text{C}\to\text{T}}(c) = p_1^{\text{C}}(c)\lambda_{\text{off}}^{\text{T}}, \tag{35}$$

where p_1^{C} is the steady-state probability to find a single particle in the channel when added from *cis* side, and $\lambda_{\text{off}}^{\text{T}}$ is the rate of exit from the pore to *trans* side. This representation is not limited to a 2MS. It is also valid, for example, for any number of Markov states inside the pore, with only one restriction – the exit rates from all the Markov states to *trans* side equal either zero or $\lambda_{\text{off}}^{\text{T}}$. The second condition of equation (31) is that not more than one particle at a time can occupy the pore, again with no specific restriction to the 2MS model. If the solute molecules are noninteracting in the solution (ideal solution), the probability to find n molecules in the channel can be given by the Poisson distribution:

$$p_n = A\frac{q^n \text{e}^{-q}}{n!}, \tag{36}$$

where A is the normalization constant, $\sum_n p_n = 1$, and q is a parameter. If the molecules do not interact also in the pore, n runs from 0 to ∞, $A = 1$ and q is the average number of molecules in the pore. In the case of no more than one molecule in the pore, then $n = 0, 1$ and $A = e^q/(1 + q)$, and one arrives at equation (30) for p_1^{C} and equation (31) for the translocation current. Methodologically, this approximation is similar to the introduction of the exclusion volume into the equation of state of ideal gas. It explains two main qualitative effects of the interaction of the molecules in the pore – the saturation of the translocation current and its asymmetry with respect to the side of addition, both can be observed and studied.

By following the latter approach, one can formally extend the model of at maximum N noninteracting molecules in the pore,

$$I_{\text{C}\to\text{T}}(c) = \frac{\sum_{n=1}^{N}\frac{(q^{\text{C}}(c))^n}{n!}}{\sum_{n=1}^{N}\frac{(q^{\text{C}}(c))^n}{n!} + 1}\frac{I_D(c)}{q^{\text{C}}(c)}. \tag{37}$$

Application

By representing the PMF as a piece-wise constant function, as shown in Figure 1, one can develop simple analytic models to illustrate (i) how is the molecule–pore interaction, (ii) how the crowding affects the translocation current, and (iii) how the kinetic rates are accessible in the electrophysiology.

We will start with a single barrier/binding site inside a pore of length L, the simplest case already discussed by other authors (see, e.g., [24,25]). Then, we will discuss a combination of a barrier and a binding site, eventually concluding with the two-barrier-one-binding-site model (TBOBS), often used to interpret the results in electrophysiology experiments [48].

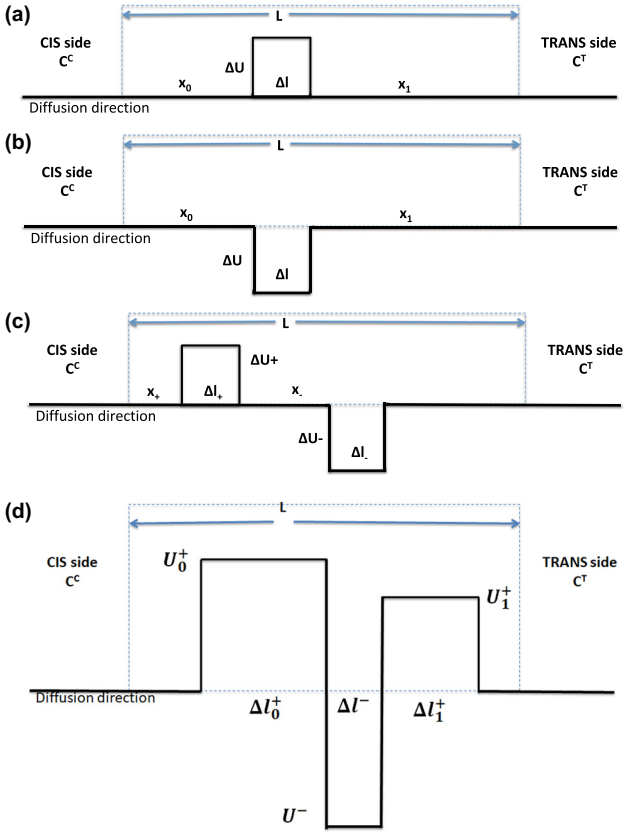

Figure 1: Schematic diagrams of a pore with (a) a single barrier PMF, (b) a single binding site PMF, (c) a barrier and a binding site PMF, and (d) a two-barriers-one-binding-site PMF. The dotted lines represent the pore length.

Analytic single barrier/binding site model

The barrier (binding site) has the width Δl and is positioned at a distance x_0 from the left entry of the pore (*cis* compartment) and x_1 from the right entry side of the pore (*trans* compartment). Let us suggest that the diffusion coefficient, D, is constant along the channel and the PMF is a rectangular function of magnitude ΔU and width Δl, located at $x = x_0$,

$$U(x) = \Delta U \mathrm{rect}\left(\frac{x - x_0}{\Delta l}\right). \tag{38}$$

Here, $\mathrm{rect}(x) = \theta(x) - \theta(x-1)$ is the rectangular functions on interval $[0, 1]$; $\theta(x)$ is the Heaviside step function.

The linear diffusion current due to the gradient of concentration c then reads

$$I_D(c) = c\frac{SD}{L}\frac{1}{(\mathrm{e}^{\Delta U/kT} - 1)\frac{\Delta l}{L} + 1}. \tag{39}$$

The molecular current is independent of the rectangle position, x_0. For the large barrier, $\Delta U \gg kT \ln(L/\Delta l)$, I_D decrease exponentially with its magnitude, while for the deep well (binding site), $\Delta U \ll -kT$, the diffusion current becomes independent on its magnitude, respectively,

$$I_D(c) = c\frac{SD}{\Delta l}\mathrm{e}^{-\Delta U/kT}; \quad \Delta U \gg kT, \tag{40}$$

$$I_D(c) = c\frac{SD}{L - \Delta l}; \quad \Delta U \ll -kT. \tag{41}$$

Thus, the presence of a barrier for the diffusing molecule decreases the diffusion current, while the binding site increases the diffusion current effectively by reducing the channel length to $L - \Delta l$.

The channel occupancy for the *cis* molecule addition, for the *trans* addition, and for the symmetric addition reads, respectively:

$$q^{\mathrm{C}}(c) = \frac{1}{2}q^{\mathrm{sym}}(c) - cS\Delta l(x_1 - x_0)\frac{\sinh\left(\frac{\Delta U}{kT}\right)}{x_0 + x_1 + \Delta l\mathrm{e}^{\Delta U/kT}}, \tag{42}$$

$$q^{\mathrm{T}}(c) = \frac{1}{2}q^{\mathrm{sym}}(c) + cS\Delta l(x_1 - x_0)\frac{\sinh\left(\frac{\Delta U}{kT}\right)}{x_0 + x_1 + \Delta l\mathrm{e}^{\Delta U/kT}}, \tag{43}$$

$$q^{\mathrm{sym}}(c) = cS(x_0 + x_1 + \Delta l\mathrm{e}^{-\Delta U/kT}). \tag{44}$$

Here, the distance to the barrier/well from the *trans* side, $x_1 \equiv L - x_0 - \Delta l$ is introduced for increasing symmetricity of the formulas.

1DD-2MS mapping, large barrier:

$$q^{\mathrm{C}}(c) = cSx_0, \quad q^{\mathrm{T}}(c) = cSx_1, \quad q^{\mathrm{sym}}(c) = cS(L - \Delta l). \tag{45}$$

Finally, the translocation current through the high barrier reads for the *cis* and the *trans* addition, respectively,

$$I_{\mathrm{C}\to\mathrm{T}}(c) = \frac{D}{\Delta l}\frac{cS\mathrm{e}^{-\Delta U/kT}}{cSx_0 + 1}; \quad I_{\mathrm{T}\to\mathrm{C}}(c) = \frac{D}{\Delta l}\frac{cS\mathrm{e}^{-\Delta U/kT}}{cSx_1 + 1}. \tag{46}$$

At high concentrations, $c \gg 1/(Sx_0)$ and $c \gg 1/(Sx_1)$, respectively, the currents reach their maximum values,

$$I^{\max}_{\mathrm{C}\to\mathrm{T}} = \frac{D}{\Delta l x_0}\mathrm{e}^{-\Delta U/kT}; \quad I^{\max}_{\mathrm{T}\to\mathrm{C}} = \frac{D}{\Delta l x_1}\mathrm{e}^{-\Delta U/kT}. \tag{47}$$

The saturated translocation current is larger when molecules are added from the side to which the barrier is closer (the barrier at the entry side).

The mapping onto the 2MS model is formal in this case, as molecules stay either on the left side of the barrier or on the right one (two different states). Thus, the obtained transition rate constants do not have real physical meaning. Nevertheless, the steady-state current, equations (46) and (47), can be used for the calculations as far as the assumption of a single (at maximum) molecule in the pore holds.

1DD-2MS mapping, strong binding:

$$q^{\mathrm{C}}(c) = cS\left(\frac{x_0 + x_1}{2} + \frac{\Delta l x_1}{x_0 + x_1}\mathrm{e}^{-\Delta U/kT}\right), \quad (48)$$

$$q^{\mathrm{T}}(c) = cS\left(\frac{x_0 + x_1}{2} + \frac{\Delta l x_0}{x_0 + x_1}\mathrm{e}^{-\Delta U/kT}\right). \quad (49)$$

The translocation current through a deep potential well reads, respectively,

$$\begin{aligned} I_{\mathrm{C}\to\mathrm{T}}(c) &= \frac{cSD}{x_0 + x_1 + cS(x_0 + x_1)^2/2 + cS\Delta l x_1 \mathrm{e}^{-\Delta U/kT}} \\ I_{\mathrm{T}\to\mathrm{C}}(c) &= \frac{cSD}{x_0 + x_1 + cS(x_0 + x_1)^2/2 + cS\Delta l x_0 \mathrm{e}^{-\Delta U/kT}}. \end{aligned} \quad (50)$$

At the high concentrations, the currents reach their maximum values,

$$\begin{aligned} I^{\max}_{\mathrm{C}\to\mathrm{T}} &= \frac{D}{(x_0 + x_1)^2/2 + \Delta l x_1 \mathrm{e}^{-\Delta U/kT}}, \\ I^{\max}_{\mathrm{T}\to\mathrm{C}} &= \frac{D}{(x_0 + x_1)^2/2 + \Delta l x_0 \mathrm{e}^{-\Delta U/kT}}. \end{aligned} \quad (51)$$

In contrast with the barrier, the saturated translocation current through the well is larger when the molecules are added from the side opposite to the well (the binding site next to the exit).

In the case of strong binding site nonadjacent to the channel ends, i.e., $x_{0,1} \neq 0$ and $U \ll kT \ln(2\Delta l x_{0,1}/(x_0 + x_1)^2)$, the 2MS model parameters,

$$K^{\mathrm{T}} = S\frac{\Delta l x_0}{x_0 + x_1}\mathrm{e}^{-\Delta U/kT}; \quad K^{\mathrm{C}} = S\frac{\Delta l x_1}{x_0 + x_1}\mathrm{e}^{-\Delta U/kT}, \quad (52)$$

$$k^{\mathrm{T}}_{\mathrm{on}} = S\frac{D}{x_1}; \quad k^{\mathrm{C}}_{\mathrm{on}} = S\frac{D}{x_0}, \quad (53)$$

$$\frac{1}{\tau_{\mathrm{res}}} = k_{\mathrm{off}} = \frac{D}{\Delta l}\frac{x_0 + x_1}{x_0 x_1}\mathrm{e}^{\Delta U/kT}. \quad (54)$$

have physical meaning. Indeed, in this case, the binding site is single and the 1DD-2MS bridging conditions, equations (32)–(34), can be satisfied for a range of concentrations from zero till the saturation.

Analytic one-barrier-one-binding site model

Let us suggest that the PMF is a sum of nonoverlapping rectangular barrier of magnitude ΔU_+ and width Δl_+, located at $x = x_+$, and rectangular well of magnitude $-\Delta U_-$ and width Δl_- located at $x = x_-$ (here, the quantities, $\Delta U_\pm$ are positive numbers, see Figure 1c),

$$U(x) = \Delta U_+ \mathrm{rect}\left(\frac{x - x_+}{\Delta l_+}\right) - \Delta U_- \mathrm{rect}\left(\frac{x - x_-}{\Delta l_-}\right). \quad (55)$$

The diffusion coefficient, D, is constant along the channel. The diffusion current due to the gradient of concentration c then reads

$$I_D(c) = c\frac{SD}{L}\frac{1}{(\mathrm{e}^{\Delta U_+/kT} - 1)\frac{\Delta l_+}{L} + (\mathrm{e}^{-\Delta U_-/kT} - 1)\frac{\Delta l_-}{L} + 1}. \quad (56)$$

The channel occupancy for the *cis* molecule addition, for the *trans* addition and for the symmetric addition, reads, respectively,

$$q^{\mathrm{C}}(c) = \frac{1}{2}q^{\mathrm{sym}}(c) - cS\frac{\Delta l_+(x_1^+ - x_0^+)\sinh\left(\frac{\Delta U_+}{kT}\right) - \Delta l_-(x_1^- - x_0^-)\sinh\left(\frac{\Delta U_-}{kT}\right) + \Delta l_+\Delta l_-\sinh\left(\frac{\Delta U_+ + \Delta U_-}{kT}\right)}{(\mathrm{e}^{\Delta U_+/kT} - 1)\Delta l_+ + (\mathrm{e}^{-\Delta U_-/kT} - 1)\Delta l_- + L}, \quad (57)$$

$$q^{\mathrm{T}}(c) = \frac{1}{2}q^{\mathrm{sym}}(c) + cS\frac{\Delta l_+(x_1^+ - x_0^+)\sinh\left(\frac{\Delta U_+}{kT}\right) - \Delta l_-(x_1^- - x_0^-)\sinh\left(\frac{\Delta U_-}{kT}\right) + \Delta l_+\Delta l_-\sinh\left(\frac{\Delta U_+ + \Delta U_-}{kT}\right)}{(\mathrm{e}^{\Delta U_+/kT} - 1)\Delta l_+ + (\mathrm{e}^{-\Delta U_-/kT} - 1)\Delta l_- + L}, \quad (58)$$

$$q^{\mathrm{sym}}(c) = cS[(\mathrm{e}^{-\Delta U_+/kT} - 1)\Delta l_+ + (\mathrm{e}^{\Delta U_-/kT} - 1)\Delta l_- + L]. \quad (59)$$

Here, the following "distances" to the barrier/well from the *trans* and *cis* sides are introduced for more symmetric formulas, $x_0^+ = x_+$; $x_1^+ = L - x_+ - \Delta l_+ - \Delta l_-$; $x_0^- = x_- - \Delta l_+$; $x_1^- = L - x_- - \Delta l_-$.

Now, we will assume that the barrier and the binding site are strong, i.e., $\Delta U_\pm \gg kT \ln(L/\Delta l_\pm)$. Then, one obtains,

$$I_D(c) = c\frac{SD}{\Delta l_+}\mathrm{e}^{-\Delta U_+/kT}. \quad (60)$$

That is, in the presence of a strong barrier, the diffusion current is independent on the binding site. The translocation current reads,

$$\begin{aligned} I_{\mathrm{C}\to\mathrm{T}}(c) &= \frac{cSD\mathrm{e}^{-\Delta U_+/kT}}{\Delta l_+ + cS\left(x_0^-\Delta l_+ + \frac{1}{2}\Delta l_-(x_1^- - x_0^-)\mathrm{e}^{(\Delta U_- - \Delta U_+)/kT}\right)}; \\ I_{\mathrm{T}\to\mathrm{C}}(c) &= \frac{cSD\mathrm{e}^{-\Delta U_+/kT}}{\Delta l_+ + cS\Delta l_+\Delta l_-\mathrm{e}^{\Delta U_-/kT}}. \end{aligned} \quad (61)$$

At high concentrations, currents reach their maximum values,

$$I^{\max}_{\mathrm{C}\to\mathrm{T}} = \frac{D\mathrm{e}^{-(\Delta U_+ + \Delta U_-)/kT}}{x_0^-\Delta l_+ \mathrm{e}^{-\Delta U_-/kT} + \frac{1}{2}\Delta l_-(x_1^- - x_0^-)\mathrm{e}^{-\Delta U_+/kT}};$$
$$I^{\max}_{\mathrm{T}\to\mathrm{C}} = \frac{D\mathrm{e}^{-(\Delta U_+ + \Delta U_-)/kT}}{\Delta l_+ \Delta l_-}. \quad (62)$$

As, $I_{\mathrm{C}\to\mathrm{T}} > I_{\mathrm{T}\to\mathrm{C}}$, we conclude that by combining a barrier with a well, the higher saturated translocation current is obtained when the barrier is closer to the entry side (where the concentration is higher) and the well on the exit side, following the addition rule of the single barrier and single-well behavior.

Markov chain model

The elementary cases discussed in the two previous subsections allows one to write down the transition rates for a more general situation of a PMF presented as a sequence of binding sites, separated by large rectangular barriers. The molecule moves in the pore by jumping between neighboring binding sites. We number the binding sites from 1 (the first site on the *cis* site) to N (the last one on the *trans* side), so that $U_k^-, \Delta l_k^-$ are the corresponding energy and the width, respectively. The barrier to the right of the binding site k has energy U_k^+ and width Δl_k^+, so that the first barrier (to enter the pore from *cis*) has number 0 and the last one (to exit to *trans*) has number N. Then, the transition rates from site k to sites $k \pm 1$ read, respectively,

$$\lambda_{kk+1} = \frac{D_k}{\Delta l_k^+ \Delta l_k^-}\mathrm{e}^{-(U_k^+ - U_k^-)/kT}, \quad (63)$$

$$\lambda_{kk-1} = \frac{D_{k-1}}{\Delta l_{k-1}^+ \Delta l_k^-}\mathrm{e}^{-(U_{k-1}^+ - U_k^-)/kT}. \quad (64)$$

Here, D_k is the diffusion constant at barrier k; $\lambda_{NN+1} = k_{\mathrm{off}}^{\mathbf{T}}$, $\lambda_{10} = k_{\mathrm{off}}^{\mathbf{C}}$. Also,

$$k_{\mathrm{on}}^{\mathbf{C}} = \frac{SD_0}{\Delta l_0^+}\mathrm{e}^{-U_0^+/kT}, \quad (65)$$

$$k_{\mathrm{on}}^{\mathbf{T}} = \frac{SD_N}{\Delta l_N^+}\mathrm{e}^{-U_N^+/kT}. \quad (66)$$

This mapping of the diffusion onto the Markov chain model assumes that the barriers are large enough for the Markov timescale conditions, like those given by equations (33)–(32), being satisfied.

By using the transition rates obtained by the Markov chain mapping, one can build a kinetic Monte-Carlo scheme [49] to simulate the translocation kinetics. This approach makes it possible to limit the occupancy for each binding site (not the whole pore), thus enhancing the possibility to study molecular crowding in the channel.

Equations (63) and (64) can be interpreted as a diffusion analog of the classical dynamic transition-state theory [26], where $D/(\Delta l^+ \Delta l^-)$ ratio replaces the frequency prefactor.

Analytic two-barriers-one-binding site model

A more realistic example is provided by the two-barrier-one-binding-site model, introduced earlier to model the transport of metabolites with binding in specific porins [22,48].

Here, Markov chain mapping formulas, (63)–(66), give (the diffusion coefficient is assumed constant along the pore for simplicity),

$$k_{\mathrm{on}}^{\mathrm{C}} = \frac{SD}{\Delta l_0^+}\mathrm{e}^{-U_0^+/kT}; \quad k_{\mathrm{on}}^{\mathrm{T}} = \frac{SD}{\Delta l_1^+}\mathrm{e}^{-U_1^+/kT}, \quad (67)$$

$$k_{\mathrm{off}}^{\mathrm{T}} = \frac{D}{\Delta l_1^+ \Delta l^-}\mathrm{e}^{-(U_1^+ - U^-)/kT}; \quad k_{\mathrm{off}}^{\mathrm{C}} = \frac{D}{\Delta l_0^+ \Delta l^-}\mathrm{e}^{-(U_0^+ - U^-)/kT}. \quad (68)$$

Then, one obtains,

$$I_D(c) = c\frac{SD}{\Delta l_0^+ \mathrm{e}^{U_0^+/kT} + \Delta l_1^+ \mathrm{e}^{U_1^+/kT}}, \quad (69)$$

$$q^{\mathrm{C}}(c) = \frac{SD\Delta l^- \mathrm{e}^{-U^-/kT}}{1 + \frac{\Delta l_0^+}{\Delta l_1^+}\mathrm{e}^{-(U_1^+ - U_0^+)/kT}},$$
$$q^{\mathrm{T}}(c) = \frac{SD\Delta l^- \mathrm{e}^{-U^-/kT}}{1 + \frac{\Delta l_1^+}{\Delta l_0^+}\mathrm{e}^{(U_1^+ - U_0^+)/kT}}. \quad (70)$$

The translocation current is given by equations (31). The maximum *cis*/*trans* asymmetry,

$$\frac{I^{\max}_{\mathrm{C}\to\mathrm{T}}}{I^{\max}_{\mathrm{T}\to\mathrm{C}}} = \frac{\Delta l_0^+}{\Delta l_1^+}\mathrm{e}^{-(U_1^+ - U_0^+)/kT}, \quad (71)$$

is determined by the magnitude and the width of the barriers.

This model contains two previous examples as special cases: (i) a symmetric case, where the barriers from the two sides are the same; (ii) a strongly asymmetric case, where the barriers are different.

Thus, in the asymmetric case, $(U_1^+ - U_0^+) \gg kT$, the results and consequences are not different from the case of a single barrier with a binding site. When the barrier heights differs less than kT, we can consider the symmetric case.

Discussion

Numerical validation

In order to show the potency of the method introduced, we considered a realistic model system, the transport of a beta-lactamase inhibitor (tazobactam) through the main porins expressed in the outer membrane of *Escherichia coli*, OmpF and OmpC. Molecules as tazobactam are used in combination with beta-lactam antibiotics because they bind strongly to beta-lactamase enzyme inhibiting them from modifying chemically antibiotics and thus revert their antibacterial efficacy [50,51]. Today, there is a wide interest in developing such inhibitors to counteract the spreading of resistant pathogens, and one common problem is to predict their transport through porins. By using multiple walkers, metadynamics simulations we reconstructed the one-dimensional free energy surface for the interaction of tazobactam with the two porins, as done for other inhibitors recently [52]. As we can see in Figure 2, the two FES profiles are a complex combination of local minima and barriers. In particular, we note a main central barrier and some minima on the positive region z (extracellular region), thus reminding the simple model of a barrier and a binding site. By calculating the diffusion current with equation (3) and thus applying equation (31), we obtained the total currents as function of gradient concentration, as reported in Figure 3.

A comparison of the two currents at constant concentration is not sufficient, as, for example, for the cis to trans current in the left panel of Figure 3. Though the barrier is lower in OmpF, than OmpC, and correspondingly larger the current, in the case of OmpF the saturation occurs before, and at concentrations higher than 10 mM, the current through OmpF becomes lower.

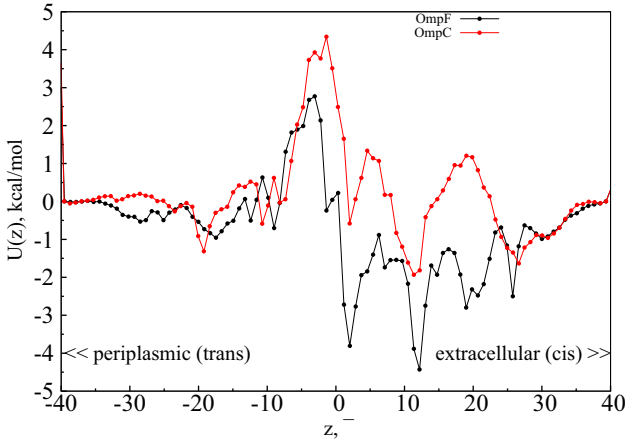

Figure 2: Free energy surface profiles vs tazobactam position along the diffusion axis inside the OmpF and OmpC porins.

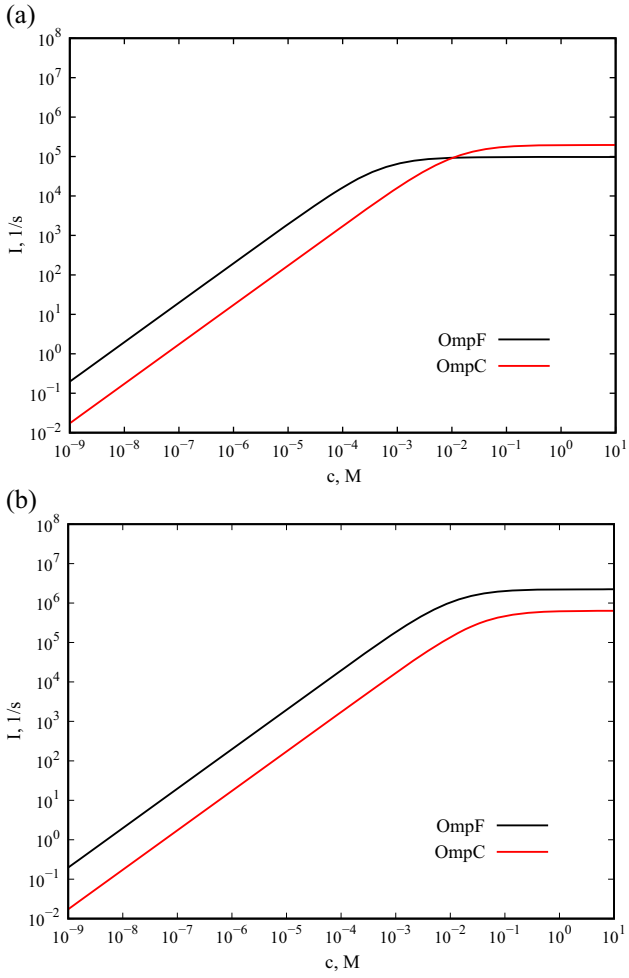

Figure 3: Current of tazobactam through the OmpF and OmpC porins versus the concentration of the molecule being added to one side only: Cis to Trans (left panel) and Trans to Cis (right panel) currents.

It is also interesting to calculate the rate of the cis → trans and trans → cis currents, as provided in Figure 4. As we illustrated with in the aforementioned simple examples, the two current are symmetric at low concentration, while at high concentration, there is an asymmetry modulated by the position of minima and barrier, see equations (57), (58), and (31):

- The current trans → cis is always superior to the cis → trans, because the highest barrier is on the trans side.
- The presence of minima is responsible for the saturation of the current at high concentration, and the change in current is more drastic on the cis → trans current because the minima are on the cis side.

Experimental validation

Our model can be employed to guide and plan experiments till the interpretation of results. A quick look at

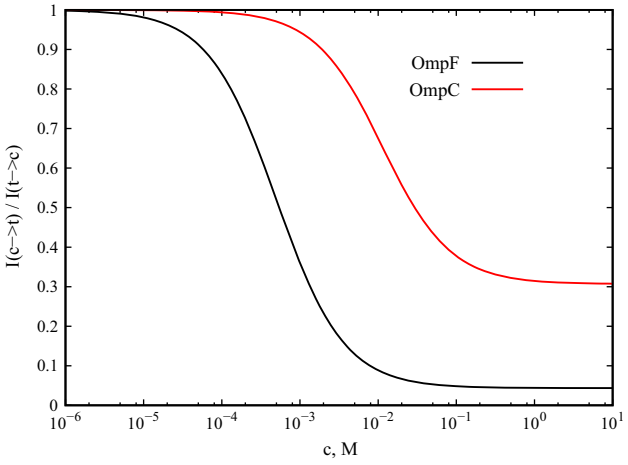

Figure 4: Ratio between the Cis to Trans and Trans to Cis current of tazobactam (being added to one side, Cis or Trans, respectively) through the OmpF and OmpC porins.

recent published data shows that kanamycin, a positively charged molecule, is transported through both OmpF/OmpC [53]. At high negative external potential applied, the association rate in OmpF saturates, contrarily to OmpC. Because kanamycin is a molecule charged positive, a high negative potential applied means to force a large association rate toward the pore, corresponding to the case described here as an increase in the gradient concentration. Interestingly, the obtained results are described by the top panel of Figure 3. Increasing more and more the external potential we would see higher association rate through OmpC than OmpF.

Further, the behavior described in Figure 4, an asymmetric transport upon asymmetric addition of molecules in solution, was measured for maltoheaxose through the maltoporin trimeric channel [21]. This sugar molecules has higher association rate when added on the trans side, exactly as for tazobactam through OmpF/OmpC. In that case, the asymmetry is visible already at 0.01 mM concentration, because of the high specificity of the maltoporin channel for sugar molecules.

Conclusion

We combined the diffusion equation with the Markov state model to obtain expression for the passive current at any concentrations, thus taking into account the effect of crowding (saturation) on transport. It is demonstrated that, in a biologically relevant case of transport of antibiotics through bacterial porins, the transition between Fick's-low regime (when the influx current is linear with the antibiotic concentration gradient) to the saturated influx current (independent on the concentration) can happen at the 0.1–1 mM concentrations. The stronger is the interaction between the molecule and the pore, the lower is the transitional concentration between the two transport regimes. This is particularly important to take into account when a model of whole-cell accumulation of molecules is designed and experimental results have to be interpreted [54].

Further, some biological conclusion can be drawn by looking at the interaction of particles inside the pores, that reflects the structural features of nanopores. For example, from the free energy profiles presented for the real case, we can conclude that by expressing these channels bacteria maximize the outward current. This means that in case of antibiotics, they can penetrate with a given inward current when present at high concentration on the cis side. Because the periplasmic space has a small volume, a low amount of molecules accumulated with the inward current are sufficient to saturate the interior [15]. However, when the external pressure of concentration disappears on the cis side, the outward current empties the periplasmic space easily. Thus, it is important to keep an almost constant external concentration for antibiotics to be effective on the small periplasmic volume.

Acknowledgements: MC thanks partial support from the Translocation consortium (http://www.translocation.com) through the IMI Joint Undertaking under grant agreement no. 115525, resources which are composed of financial contribution from the European Union's seventh framework programme (FP7/2007-2013) and EFPIA companies' kind contribution. IVB acknowledges the financial support by DAAD (Deutscher Akademischer Austausch Dienst) during his research stay period at Jacobs University Bremen. SM is funded through the bilateral Russian (RFBR)-Italian(CNR) research project No. 20-58-7802(RFBR) and B55F21000620005 (CNR). The authors gratefully acknowledge the computing time granted through the ISCRA-B project "PREDICT" on the supercomputer Marconi100 at CINECA, IT.

Conflict of interest: The authors state no conflict of interest.

Data availability statement: The datasets generated during and/or analyzed during the current study are available from the corresponding author on reasonable request.

References

[1] Vergalli J, Bodrenko IV, Masi M, Moynié L, Acosta-Gutierrez S, Naismith JH, et al. Porins and small-molecule translocation across the outer membrane of Gram-negative bacteria. Nature Rev Microbiol. 2019 Dec;33(3):1831–913.

[2] Ujwal R, Cascio D, Colletier JP, Faham S, Zhang J, Toro L, et al. The crystal structure of mouse VDAC1 at 2.3 Åresolution reveals mechanistic insights into metabolite gating. Proc National Acad Sci. 2008;105(46):17742–7.

[3] van den Berg B, Prathyusha Bhamidimarri S, Dahyabhai Prajapati J, Kleinekathöfer U, Winterhalter M. Outer-membrane translocation of bulky small molecules by passive diffusion. Proc National Acad Sci. 2015 Jun;112(23):E2991–9. Available from: http://www.pnas.org/lookup/doi/10.1073/pnas.1424835112.

[4] Biswas S, Mohammad MM, Patel DR, Movileanu L, van den Berg B. Structural insight into OprD substrate specificity. Nature Struct & Mol Biol. 2007 Nov;14(11):1108–9.

[5] Ferrara LGM, Wallat GD, Moynié L, Dhanasekar NN, Aliouane S, Acosta-Gutierrez S, et al. MOMP from campylobacter jejuni is a trimer of 18-stranded β-barrel monomers with a Ca(2+) ion bound at the constriction zone. J Mol Biol. 2016 Nov;428(22):4528–43.

[6] Pathania M, Acosta-Gutierrez S, Bhamidimarri SP, Baslé A, Winterhalter M, Ceccarelli M, et al. Unusual constriction zones in the major Porins OmpU and OmpT from Vibrio cholerae. Structure. 2018;26(5):708–21.

[7] Acosta-Gutierrez S, Ferrara L, Pathania M, Masi M, Wang J, Bodrenko I, et al. Getting drugs into gram-negative bacteria: Rational rules for permeation through general porins. ACS Infect Diseases. 2018 Aug;4(10):1487–98.

[8] Marbach S, Dean DS, Bocquet Lxr. Transport and dispersion across wiggling nanopores. Nature Phys. 2018 Jul;14(11):1–6.

[9] Gravelle S, Joly L, Ybert C, Bocquet L. Large permeabilities of hourglass nanopores: from hydrodynamics to single file transport. J Chem Phys. 2014 Nov;141(18):18C526.

[10] Willems K, Van Meervelt V, Wloka C, Maglia G. Single-molecule nanopore enzymology. Philosoph Trans R Soc London B Biol Sci. 2017 Aug;372(1726):20160230.

[11] Chowdhury R, Ren T, Shankla M, Decker K, Grisewood M, Prabhakar J, et al. PoreDesigner for tuning solute selectivity in a robust and highly permeable outer membrane pore. Nature Commun. 2018 Sep;9(1):3661–10.

[12] Qing Y, Ionescu SA, Pulcu GS, Bayley H. Directional control of a processive molecular hopper. Science. 2018 Aug;361(6405):908–12.

[13] Ouldali H, Sarthak K, Ensslen T, Piguet F, Manivet P, Pelta J, et al. Electrical recognition of the twenty proteinogenic amino acids using an aerolysin nanopore. Nature Biotechnol. 2020 Jan;38:1–10.

[14] Richter MF, Drown BS, Riley AP, Garcia A, Shirai T, Svec RL, et al. Predictive compound accumulation rules yield a broad-spectrum antibiotic. Nature Publishing Group. 2017 May;545(7654):299–304.

[15] Brönstrup HPVFSKHMAGRAHM, Fetz V, Hotop Sk, García-Rivera MA, Heumann A, Brönstrup M. Quantification of uptake in gram-negative bacteria. Anal Chem. 2018 Nov;91(3):1863–72.

[16] Masi M, Réfrégiers M, Pos KM, Pagès JM. Mechanisms of envelope permeability and antibiotic influx and efflux in Gram-negative bacteria. Nature Microbiol. 2017 Feb;2(3):17001–7.

[17] Westfall DA, Krishnamoorthy G, Wolloscheck D, Sarkar R, Zgurskaya HI, Rybenkov VV. Bifurcation kinetics of drug uptake by Gram-negative bacteria. PLoS One. 2017 Sep;12(9):e0184671.

[18] Saha P, Sikdar S, Krishnamoorthy G, Zgurskaya HI, Rybenkov VV. Drug Permeation against efflux by two transporters. ACS Infect Diseases. 2020 Feb;6:747–58.

[19] Hänggi P, Talkner P, Borkovec M. Reaction-rate theory: fifty years after Kramers. Rev Mod Phys. 1990 Apr;62(2):251–341. Available from: https://link.aps.org/doi/10.1103/RevModPhys.62.251.

[20] Nestorovich EM, Danelon C, Winterhalter M, Bezrukov SM. Designed to penetrate: time-resolved interaction of single antibiotic molecules with bacterial pores. Proc Nat Acad Sci US Am. 2002 Jul;99(15):9789–94.

[21] Kullman L, Winterhalter M, Bezrukov SM. Transport of maltodextrins through maltoporin: a single-channel study. Biophys J. 2002 Feb;82(2):803–12. Available from: http://eutils.ncbi.nlm.nih.gov/entrez/eutils/elink.fcgi?dbfrom=pubmed&id=11806922&retmode=ref&cmd=prlinks.

[22] Schwarz G, Danelon C, Winterhalter M. On translocation through a membrane channel via an internal binding site: kinetics and voltage dependence. Biophys J. 2003 May;84(5):2990–8.

[23] Ghai I, Pira A, Scorciapino MA, Bodrenko I, Benier L, Ceccarelli M, et al. General method to determine the flux of charged molecules through nanopores applied to beta-lactamase inhibitors and OmpF. J Phys Chem Lett. 2017 mar;8(6):1295–301. Available from: http://pubs.acs.org/doi/10.1021/acs.jpclett.7b00062.

[24] Bauer WR, Nadler W. Molecular transport through channels and pores: effects of in-channel interactions and blocking. Proc National Acad Sci. 2006;103(31):11446–51. Available from: https://www.pnas.org/content/103/31/11446.

[25] Bezrukov SM, Berezhkovskii AM, Szabo A. Diffusion model of solute dynamics in a membrane channel: mapping onto the two-site model and optimizing the flux. J Chem Phys. 2007;127(11):115101. Available from: https://doi.org/10.1063/1.2766720.

[26] Kramers HA. Brownian motion in a field of force and the diffusion model of chemical reactions. Physica. 1940 Apr;7(4):284–304. Available from: http://linkinghub.elsevier.com/retrieve/pii/S0031891440900982.

[27] Gardiner CW. Handbook of Stochastic Methods for Physics, Chemistry, and the Natural Sciences. Berlin: Springer; 2004.

[28] Landau LD, Lifshitz EM, Pitaevskiĭ LP, Sykes JB, Kearsley M, Statistical Physics. Part 1 3rd ed. Amsterdam; London: Elsevier Butterworth Heinemann; 2008. Published in 2 parts.

[29] Zwanzig R. Diffusion past an entropy barrier. J Phys Chem. 1992 May;96(10):3926–30. Available from: http://pubs.acs.org/doi/abs/10.1021/j100189a004.

[30] Kalinay P, Percus JK. Corrections to the Fick-Jacobs equation. Phys Rev E. 2006 Oct;74(4):041203. Available from: https://link.aps.org/doi/10.1103/PhysRevE.74.041203.

[31] Bradley RM. Diffusion in a two-dimensional channel with curved midline and varying width: Reduction to an effective

one-dimensional description. Phys Rev E. 2009 Dec;80(6):061142. Available from: https://link.aps.org/doi/10.1103/PhysRevE.80.061142.
[32] Berezhkovskii A, Szabo A. Time scale separation leads to position-dependent diffusion along a slow coordinate. J Chem Phys. 2011 Aug;135(7):074108. Available from: http://aip.scitation.org/doi/10.1063/1.3626215.
[33] Berezhkovskii AM, Pustovoit MA, Bezrukov SM. Channel-facilitated membrane transport: Transit probability and interaction with the channel. J Chem Phys. 2002 June;116(22):9952–6. Available from: http://aip.scitation.org/doi/10.1063/1.1475758.
[34] Stratonovich RL. Radiotekh Elektron (Moscow). 1958;3:497.
[35] Reguera D, Luque A, Burada PS, Schmid G, Rubí JM, Hänggi P. Entropic splitter for particle separation. Phys Rev Lett. 2012 Jan;108(2):020604. Available from: https://link.aps.org/doi/10.1103/PhysRevLett.108.020604.
[36] Acosta-Gutierrez S, Bodrenko IV, Ceccarelli M. The influence of permeability through bacterial porins in whole-cell compound accumulation. Antibiotics (Basel, Switzerland) 2021 May;10(6):635. Available from: https://www.mdpi.com/2079-6382/10/6/635/htm.
[37] Im W, Roux B. Ion permeation and selectivity of OmpF Porin: A theoretical study based on molecular dynamics, brownian dynamics, and continuum electrodiffusion theory. J Mol Biol. 2002 Sep;322(4):851–69. Available from: http://www.sciencedirect.com/science/article/pii/S0022283602007787, http://linkinghub.elsevier.com/retrieve/pii/S0022283602007787.
[38] Hummer G. Position-dependent diffusion coefficients and free energies from Bayesian analysis of equilibrium and replica molecular dynamics simulations. New J Phys. 2005 Feb;7:34. Available from: http://stacks.iop.org/1367-2630/7/i=1/a=034?key=crossref.e1c728f07773a70730fc6b9bedef5646.
[39] Wilson MA, Nguyen TH, Pohorille A. Combining molecular dynamics and an electrodiffusion model to calculate ion channel conductance. J Chem Phys. 2014 Dec;141(22):22D519. Available from: http://aip.scitation.org/doi/10.1063/1.4900879.
[40] Berezhkovskii AM, Makarov DE. Communication: coordinate-dependent diffusivity from single molecule trajectories. J Chem Phys. 2017 Nov;147(20):201102. Available from: http://aip.scitation.org/doi/10.1063/1.5006456.
[41] Torrie GM, Valleau JP. Monte Carlo free energy estimates using nonBoltzmann sampling: Application to the sub-critical Lennard-Jones fluid. Chem Phys Lett. 1974 Oct;28(4):578–81. Available from: http://linkinghub.elsevier.com/retrieve/pii/0009261474801090.
[42] Laio A, Parrinello M. Escaping free-energy minima. Proc Natl Acad Sci. 2002 Oct;99(20):12562–6. Available from: http://www.jstor.org/stable/3073262, http://www.pnas.org/cgi/doi/10.1073/pnas.202427399.
[43] Tiwary P, Parrinello M. From metadynamics to dynamics. Phys Rev Lett. 2013 Dec;111(23):230602. Available from: https://link.aps.org/doi/10.1103/PhysRevLett.111.230602.
[44] Acosta-Gutierrez S, Scorciapino MA, Bodrenko IV, Ceccarelli M. Filtering with electric field: the case of E. coli porins. J Phys Chem Lett. 2015 May;6(10):1807–12. Available from: http://pubs.acs.org/doi/10.1021/acs.jpclett.5b00612.
[45] D'Agostino T, Salis S, Ceccarelli M. A kinetic model for molecular diffusion through pores. Biochim Biophys Acta - Biomembr. 2016 Jul;1858(7):1772–7. Available from: doi: http://dx.doi.org/10.1016/j.bbamem.2016.01.004, http://linkinghub.elsevier.com/retrieve/pii/S0005273616000055.
[46] Bajaj H, Acosta Gutierrez S, Bodrenko I, Malloci G, Scorciapino MA, Winterhalter M, et al. Bacterial outer membrane porins as electrostatic nanosieves: exploring transport rules of small polar molecules. ACS Nano. 2017 Jun;11(6):5465–73. Available from: http://pubs.acs.org/doi/10.1021/acsnano.6b08613.
[47] Colquhoun D, Hawkes AG. Relaxation and fluctuations of membrane currents that flow through drug-operated channels. Proc R Soc B Biol Sci. 1977 Nov;199(1135):231–62.
[48] Nekolla S, Andersen C, Benz R. Noise analysis of ion current through the open and the sugar-induced closed state of the LamB channel of Escherichia coli outer membrane: evaluation of the sugar binding kinetics to the channel interior, Biophys J. 1994 May;66(5):1388–97.
[49] Ceccarelli M, Vargiu AV, Ruggerone P. A kinetic Monte Carlo approach to investigate antibiotic translocation through bacterial porins. J Phys Condensed Matter Inst Phys J. 2012 Mar;24(10):104012.
[50] Papp-Wallace KM. The latest advances in beta-lactam/beta-lactamase inhibitor combinations for the treatment of Gram-negative bacterial infections. Expert Opinion Pharmacotherapy. 2019 Nov;20(17):2169–84. Available from: https://doi.org/10.1080/14656566.2019.1660772.
[51] Davies DT, Leiris S, Zalacain M, Sprynski N, Castandet J, Bousquet J, et al. Discovery of ANT3310, a novel broad-spectrum serine beta-Lactamase inhibitor of the Diazabicyclooctane class, which strongly potentiates meropenem activity against Carbapenem-resistant enterobacterales and Acinetobacter baumannii. J Med Chem. 2020 Dec;63(24):15802–20. Available from: https://pubs.acs.org/doi/10.1021/acs.jmedchem.0c01535.
[52] Pira A, Scorciapino MA, Bodrenko IV, Bosin A, Acosta-Gutierrez S, Ceccarelli M. Permeation of beta-Lactamase inhibitors through the general porins of gram-negative bacteria. Molecules 2020 Dec;25(23):5747.
[53] Bafna JA, Sans-Serramitjana E, Acosta-Gutierrez S, Bodrenko IV, Hörömpöli D, Berscheid A. Kanamycin uptake into Escherichia coli is facilitated by OmpF and OmpC Porin channels located in the outer membrane. ACS Infect Diseases. 2020 Jul;6(7):1855–65.
[54] Zgurskaya HI, Rybenkov VV. Permeability barriers of Gram-negative pathogens. Ann NY Acad Sci. 2020 Jan;1459(1):5–18.